Vibrational Dynamics in Dendridic Oligoarylamines by Raman Spectroscopy and Incoherent Inelastic Neutron Scattering

ARTICLE *in* THE JOURNAL OF PHYSICAL CHEMISTRY B · APRIL 2014

Impact Factor: 3.3 · DOI: 10.1021/jp502735s · Source: PubMed

8 AUTHORS, INCLUDING:

Guy Louarn
University of Nantes
203 PUBLICATIONS **3,612** CITATIONS
SEE PROFILE

David Djurado
French National Centre for Scientific Research
140 PUBLICATIONS **1,803** CITATIONS
SEE PROFILE

Stéphane Rols
Institut Laue-Langevin
151 PUBLICATIONS **1,837** CITATIONS
SEE PROFILE

Adam Pron
Warsaw University of Technology
345 PUBLICATIONS **8,099** CITATIONS
SEE PROFILE

THE JOURNAL OF PHYSICAL CHEMISTRY B

Article

pubs.acs.org/JPCB

Vibrational Dynamics in Dendridic Oligoarylamines by Raman Spectroscopy and Incoherent Inelastic Neutron Scattering

Irena Kulszewicz-Bajer,*[,†] Guy Louarn,*[,‡] David Djurado,[§] Lukasz Skorka,[†] Marek Szymanski,[§,⊥] Jean Yves Mevellec,[‡] Stephane Rols,[∥] and Adam Pron[†]

[†]Faculty of Chemistry, Warsaw University of Technology, Noakowskiego 3, 00-664 Warsaw, Poland

[‡]Insitut des Materiaux Jean Rouxel, CNRS-University of Nantes, 2 rue de la Houssinier, 44322 Nantes, France

[§]University Grenoble Alpes, INAC-SPrAM; CNRS, INAC-SPrAM; CEA, INAC-SPrAM, F-38000 Grenoble, France

[∥]Institut Laue Langevin, 6 rue J. Horovitz, 38042 Grenoble, France

Supporting Information

ABSTRACT: Vibrational dynamics in triarylamine dendrimers was studied in a complementary way by Raman and infrared (IR) spectroscopies and incoherent inelastic neutron scattering (IINS). Three molecules were investigated, namely, unsubstituted triarylamine dendrimer of the first generation and two dendrimers of the first and second generation, substituted in the crown with butyl groups. To facilitate the assignment of the observed IR and Raman modes as well as the IINS peaks, vibrational models, based on the general valence force field method (GVFF), were calculated for all three compounds studied. A perfect consistency between the calculated and experimental results was found. Moreover, an important complementarity of the vibrational spectroscopies and IINS was established for the investigated dendrimers. The IINS peaks originating mainly from the C−H motions were not restricted by particular selection rules and only dependent on the IINS cross section. To the contrary, Raman and IR bands were imposed by the selection rules and the local geometry of the dendrimers yielding mainly C−C and C−N deformation modes with those of C−H nature of much lower intensity. Raman spectroscopy was also applied to the studies of the oxidation of dendrimers to their cationic forms. A strong Raman resonance effect was observed, since the spectra of the studied compounds, registered at different levels of their oxidation, strongly depended on the position of the excitation line with respect to their electronic spectrum. In particular, the blue (458 nm) excitation line turned out to be insensitive toward the cationic forms yielding very limited spectral information. To the contrary, the use of the red (647 nm) and infrared (1064 nm) excitation lines allowed for an unambiguous monitoring of the spectral changes in dendrimers oxidized to nominally monocationic and tricationic states. The analysis of oxidation-induced spectral changes in the tricationic state indicated that the charge storage configuration predominantly involved one spinless dication of the quinoid bond sequence and one radical cation. However, small numbers of dications were also found in a nominally monocationic state, where only radical cations should have been present. This finding was indicative of some inhomogeneity of the oxidation.

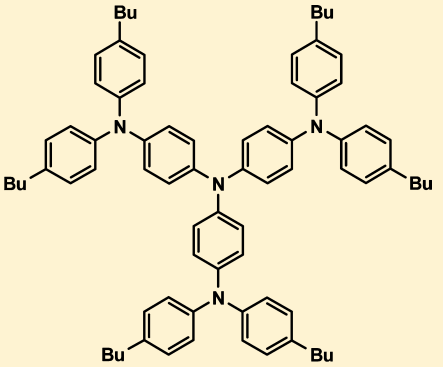

INTRODUCTION

The triarylamine moiety is a widely used building block for a variety of functional materials used in organic and hybrid (organic/inorganic) electronics,[1−6] optoelectronics,[7−22] and electrochemical devices.[23−27] Linear and branched triarylamine homooligomers as well as their polymeric analogues are frequently used as active materials in p-channel organic field effect transistors (OFETs), since they combine reasonably high hole mobilities with amorphous structure, the latter facilitating the formation of structurally homogeneous films by solution processing.[3,5] Cyclic triarylamines, in turn, readily crystallize to yield anisotropic layers of columnar-type supramolecular organization.[28] Besides their use as active layers in OFETs, both low and high molecular weight triarylamine derivatives serve as hole injection and hole transporting layers in organic light emitting diodes (OLEDs),[16−21] including the first reported multilayer OLED.[29]

Dendridic oligoarylamines constitute a special class of this family of organic conductors. They have been studied for nearly 25 years[30−33] due to the peculiar topology of their macromolecules and the capability of forming spin-delocalized, stable multicationic states.[34−37]

Molecular dynamics of neutral and polycationic triarylamine dendrons deposited as thin films is of fundamental interest, since it is closely related to their redox, magnetic, and electrical transport properties. Raman spectroscopy and incoherent inelastic neutron scattering (IINS) are convenient and

Received: March 19, 2014
Revised: April 25, 2014

   dx.doi.org/10.1021/jp502735s | J. Phys. Chem. B XXXX, XXX, XXX−XXX

Scheme 1. Structural Formulae of the First and Second Generation Triarylamine Dendrimers Studied

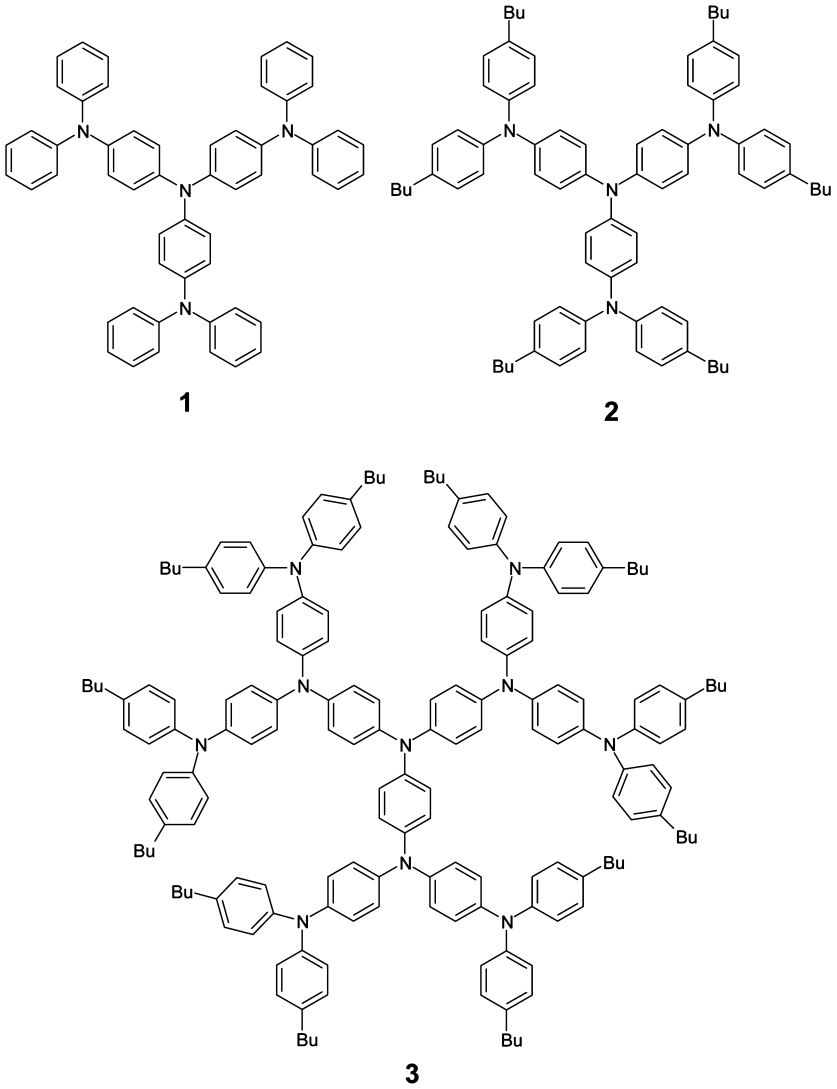

complementary tools for studying vibrational properties of such molecules. Raman spectroscopy gives a high energy resolution and is very sensitive to electronic and optical properties of molecules under study. IINS by contrast has a lower energy resolution, but it is not sensitive to the presence of electrons and gives access to all vibrational modes of the system without any selection rule.[38] Raman studies of thin layers of triarylamine dendrimers, reported to date, are scarce and limited to the studies of the effect of annealing of thin arylamine films on their spectra obtained with one excitation line.[39−41] To the best of our knowledge, incoherent inelastic neutron scattering investigations have never been reported for this class of organic semiconductors. In this paper, we present a theoretically calculated vibrational model for first and second generation triarylamine dendrons and confront it with experimental data derived from Raman and neutron scattering studies.

RESULTS AND DISCUSSION

Neutral Dendrimers. The studied dendridic triarylamines are depicted in Scheme 1.

1 has already been reported,[33] and **2** and **3** were also described, however, with different alkyl or alkoxy substituents.[33,37,42] For this reason, the applied synthetic pathways will not be discussed here. Readers interested in the details of the synthesis are referred to ref 42.

Raman spectra of low and high molecular weight aromatic amines, both in their neutral and oxidized (cationic) states, are very sensitive toward the energy of the excitation line which is caused by resonance effects, frequently interfering in the measurements.[43,44] Therefore, registration of the spectra obtained with excitation lines of different energy, λ_{exc}, is highly desirable. In Figures 1 and 2, Raman spectra of **1** and **2**, registered for λ_{exc} of decreasing energy, are compared.

In the UV−vis spectra of neutral **1** and **2**, no band giving rise to a significant value of absorbance above 400 nm can be distinguished (*vide infra*). This means that the resonance effect is expected for none of the applied excitation line. Although the positions of the observed Raman bands do not vary with the energy of the excitation line, the quality of the spectrum, determined by the signal-to-noise ratio, is strongly dependent on λ_{exc}. It increases with decreasing energy of the excitation line, being the best for λ_{exc} = 647 nm (red line). For the IR excitation line (λ_{exc} = 1064 nm), the spectrum quality worsens again. Only a low resolution spectrum of the neutral form has been registered for **3** (Figure 3); see also Table 1.

dx.doi.org/10.1021/jp502735s | J. Phys. Chem. B XXXX, XXX, XXX−XXX

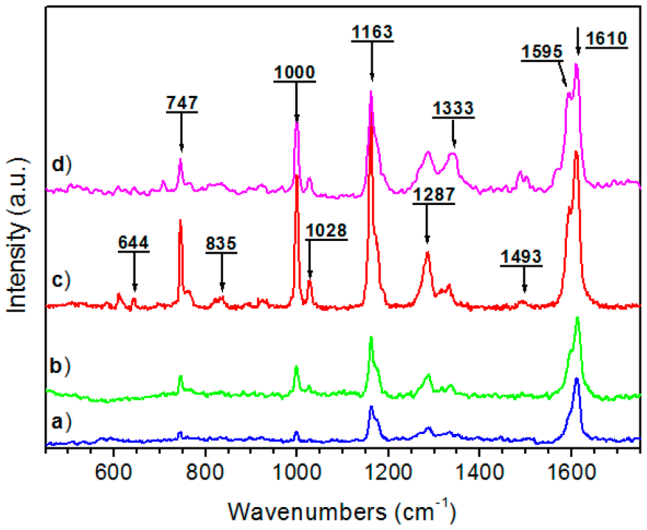

Figure 1. Raman spectra of neutral arylamine dendrimer **1** registered using different excitation lines: (a) blue line 458 nm; (b) green line 514 nm; (c) red line 647 nm; d) Fourier transform Raman spectrum, infrared line 1064 nm.

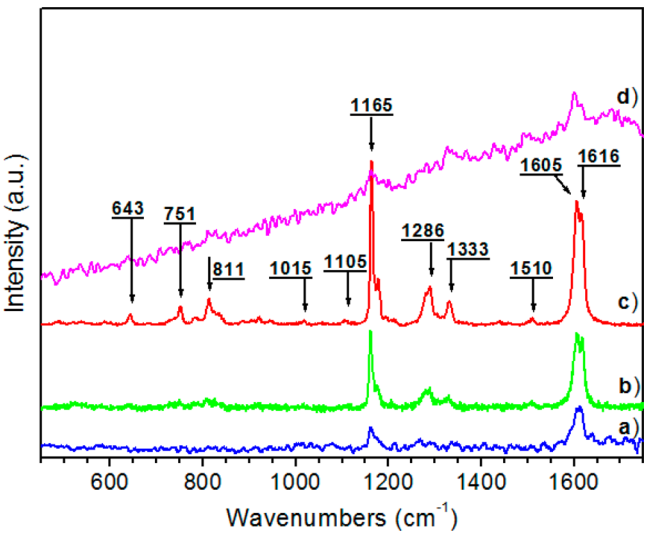

Figure 2. Raman spectra of neutral arylamine dendrimer **2** registered using different excitation lines: (a) blue line 458 nm; (b) green line 514 nm; (c) red line 647 nm; (d) Fourier transform Raman spectrum, infrared line 1064 nm.

We will focus here on a comparative discussion of the spectra of **1** and **2** registered with λ_{exc} = 647 nm. There are some common Raman lines in both spectra. In particular, two strongly overlapping, sharp peaks at 1595 and 1610 cm^{-1} can unambiguously be assigned to the C−C stretching deformations in the benzenoid type of ring, consistent with the reduced neutral state of **1** and **2** in which all aromatic rings are *quasi*-equivalent and benzenoid in nature. A clear band at 1289 cm^{-1}, which is usually attributed to the C−N stretching in aromatic amines,[40,45,46] is also characteristic of the neutral state of **1** and **2**. A weak band at ca. 1175 cm^{-1} together with a strong band at ca. 1162 cm^{-1} are characteristic of the C−H in-plane bending deformations in the aromatic ring. Finally, a weak intensity peak at ca. 820−825 cm^{-1} should be attributed to the deformations of the amine group; i.e., its presence corroborates the neutral state of both molecules. In the spectrum of **1**, three additional

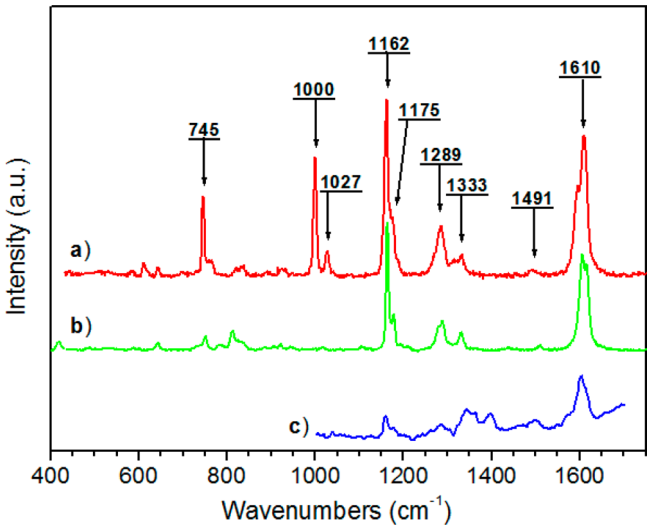

Figure 3. Raman spectra of neutral arylamine dendrimers registered using different excitation lines: (a) dendrimer **1** (647 nm); (b) dendrimer **2** (647 nm); (c) dendrimer **3** (1064 nm, Fourier transform Raman spectrum).

lines can be found which are absent in the spectrum of **2**, at 1027, 1000, and 745 cm^{-1}. They are characteristic of C−H deformations in monosubstituted benzene rings,[46,47] and their presence confirms the coexistence of monosubstituted and *para*-substituted rings in **1**. In the spectrum of **2**, a very weak band can be noticed at 1448 cm^{-1}, i.e., in the spectral range characteristic of CH_2/CH_3 deformations of the aliphatic groups. In aromatic amines or conjugated molecules (macromolecules), the aliphatic bands are very weak, especially under resonance conditions. Therefore, we tend to ascribe this band to the CH_2/CH_3 in the butyl substituent. There are two additional findings which further support this attribution: (i) this band is absent in the spectrum of **1** (unsubstituted analogue of **2**); (ii) it remains unchanged upon oxidation of the molecule being clearly detectable in the spectra of the oxidized forms of **2** (*vide infra*).

Close inspection of the spectra of **1** and **2** reveals the presence of additional bands of low intensity which cannot be assigned to the vibrations of neutral arylamine molecules, in their reduced state. A weak band in the vicinity of 1480−1500 cm^{-1} can tentatively be ascribed to C═N stretching.[48] This attribution is reasonable, since both **1** and **2** are very sensitive to oxidation; thus, minute amounts of these compounds could be partially oxidized upon their dissolution and film casting. A weak peak at 1333 cm^{-1} should in turn be ascribed to the presence of very small amounts of radical cations characteristic of the first oxidation step of **1** and **2**.[48] One should not attempt to perform any type of quantitative estimation of the fraction of the oxidized forms of **1** and **2** in the studied samples, since bands originating from the vibrations of the oxidized parts of the molecule are resonantly enhanced when λ_{exc} = 647 nm (red line) is used. This resonance enhancement is even more pronounced in the spectrum of **1** obtained with the IR excitation line (λ_{exc} = 1064 nm) where the intensity of lines assigned to the oxidized form relatively increases (see Figure 1d). This problem will be discussed in detail in a subsequent part of the paper.

To confront the obtained experimental spectra of the studied dendrimers with theoretical predictions, we have elaborated their vibrational models. The applied calculation methodology

dx.doi.org/10.1021/jp502735s | J. Phys. Chem. B XXXX, XXX, XXX−XXX

Table 1. Calculated and Experimentally Measured Frequencies (in cm^{-1}) of the Main Vibrational Modes of 1, 2, and 3 in Their Neutral Form

benzene	dendrimer 1 exptl bands				dendrimer 2 exptl bands			dendrimer 3 exptl bands	
Wilson notation[54]	IINS	Raman	FTIR	calcd modes	IINS	Raman	FTIR	Raman	assignments [47,55]
1596 (8a)	1600	1610		1616		1616		1616	ring stretch
1596 (8b)		1595	1587	1624		1605	1607		ring stretch
1486 (19a)	1487	1493	1488	1489		1510	1496	1499	ring stretch + deformation
butyl gr.					1455	1439	1465		methyl and methylene H−C−H def.
doping		1333				1333		1344	radical cation (residual)
butyl gr.					1300		1310		in-plane methylene twisting−rocking
1326 (3)	1300	1310	1310	1310			1305		ring stretch
		1287		1280		1286	1263	1280	C−N stretch + ring stretch
1178 (9a)	1165	1163		1166	1178	1165	1178	1165	ring C−H deformation
1038 (18b)				1102	1108	1105	1113		aromatic C−H bend
1038 (18a)	1022	1028		1020	1010	1015	1015		C−H deformation
1010 (12)		1000		996					ring deformation
975 (17a)	968			966-	942				C−H deformation (out of plane)
849 (10a)	832	835	820	829	822	811	821		C−H deformation (out of plane)
673 (11)	752	747	750	747	733	751			C−H deformation (out of plane)
703 (4)	700		691	693					ring deformation (out of plane)
606 (6b)	617	644		648	625	643			ring deformation
410 (16a)	411			423	415	418			ring deformation (out of plane)

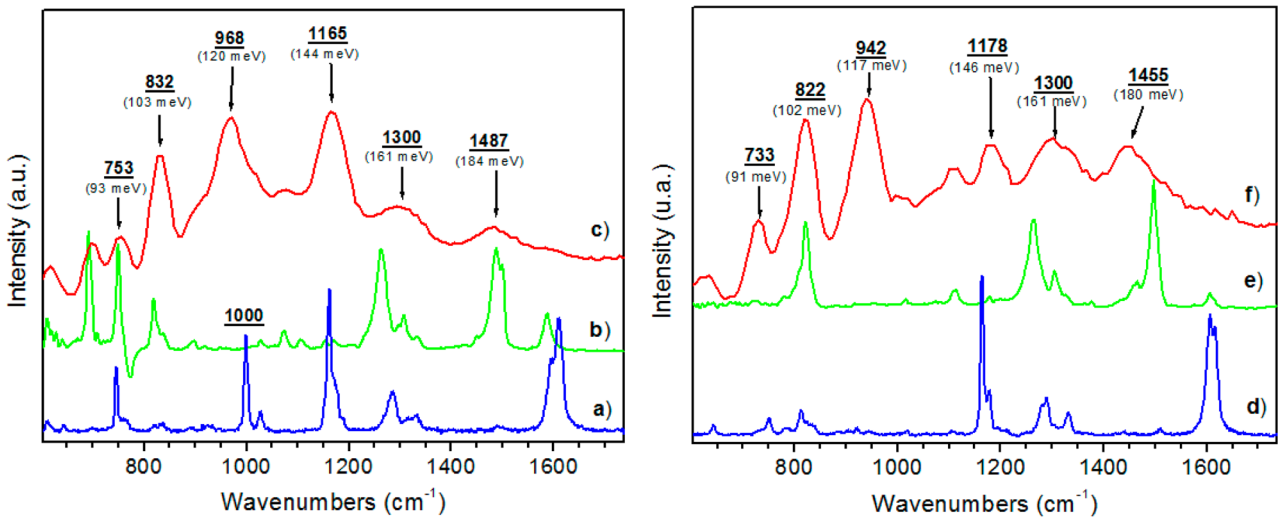

Figure 4. Vibrational spectra of dendrimer **1** (left) and dendrimer **2** (right): (a and d) Raman scattering (red excitation); (b and e) IR absorption; (c and f) inelastic incoherent neutron scattering.

has previously been tested with success in elaborating vibrational models of electroactive molecules and macromolecules,[46,49] including aromatic amines.[50] Its detailed description can be found in ref 51; here, we only briefly outline it. The force field and frequencies are determined using the Fourier dynamic matrix. The calculations require the knowledge of bond lengths, bond angles, and force constants. To obtain the former, it is necessary to optimize the molecule geometry, which is usually done by applying semiempirical or *ab initio* quantum chemistry methods depending on the complexity of the studied molecules. In our case, it is carried out with the Hyperchem 75 software (semiempirical method: PM3). An internal coordinate system is used to compute the fundamental vibrations of the studied molecules. Local redundancies can be handled by suitable symmetry coordinates. The calculations start from a minimal set of force constants, expressed in terms of internal coordinates. It is necessary to assume that certain force constants must be fairly local, i.e., only dependent on the nearest chemical environment. For this reason, they can be transferred from model compounds of simpler topology. Using this procedure, the number of force constants used in the calculations can be minimized, which leads to a significant reduction of the number of independent parameters. These parameters are finally adjusted from the experimental and calculated frequencies with a least-squares method. The calculated bond lengths and angles between bonds, derived from the optimized geometry, as well as the obtained main force constants (FG matrix) and modeling Cartesian displacements of the main experimental modes are listed in the Supporting Information (Chart S1). The measured and calculated modes, together with their assignment, are listed in Table 1.

dx.doi.org/10.1021/jp502735s | J. Phys. Chem. B XXXX, XXX, XXX−XXX

On the basis of our semiempirical modeling, the three studied dendrimers have at least a C_3 symmetry. The phenyl rings are assumed to be flat and identical to each other, with fixed C−C (1.409 Å) and C−H (1.078 Å) distances and ∠CCC angles and ∠CCH angles of exactly 120°. The values for the bond lengths are the averaged values as obtained from our modeling, and from spectroscopic and X-ray crystallographic studies of TPA (triphenylamine) in the solid state.[52,53] Then there are only three other parameters left that are allowed to vary, i.e., the C−N distance (taken as 1.421 Å), the φ angle by which the phenyl groups are rotated around the C−N bonds, and the ∠CNC angle. The angles are defined in such a manner that a fully planar geometry of TPA means $\varphi = 0$ and ∠CNC = 120°. If ∠CNC is exactly120°, an additional C_2 symmetry axis exists, passing through each of the three phenyl rings, yielding a D_3 symmetry for the molecule. Our modeling gives a φ angle somewhere between 40 and 60° and a ∠CNC angle between 119 and 120°, the values similar to those previously obtained for triaryl amine derivatives.[52,53] This φ angle likely changes during the oxidation process. Since we cannot exclude the impact of this torsion on the position and the intensity of some vibrational modes, we assume that this evolution only concerns modes with very low frequencies (<600 cm^{-1}). Above this frequency, modes are mainly due to valence bond stretchings or bendings and the contribution of the torsion or twist is negligible. In addition, it should be stressed here that all nitrogen atoms in the dendrimer structures are located in the same plane. More details can be found in the Supporting Information.

These considerations concerning the symmetries of the dendrimers are very important in regard to the selection rules and the relative intensities of IINS, IR, and Raman bands. In Figure 4, where the vibrational data of **1** and **2** are presented on the same graph, the complementarity of these spectroscopies can easily be noticed. For instance, the Raman and IR spectra present mainly two lines in the 1400−1700 cm^{-1} range, assigned to C−C stretching deformations and pointed in **1** at 1610 and 1493 cm^{-1}. These peaks can be ascribed without ambiguities to 8a and 19a modes in Wilson notation. These modes are weakly active in the IINS spectra, due to the low contribution of the CH motions. On the contrary, the in-plane and out-of-plane CH-bending modes, well-known as modes 9a and 10a in Wilson notation, can be observed with a high intensity in the IINS spectra at 1165 and 832 cm^{-1} (144 and 103 meV). The intense peaks pointed at 968 and 942 cm^{-1} in the IINS of **1** and **2**, respectively, fully absent in Raman and IR spectra, deserve some discussion. As already written above, in contrast to the Raman and IR spectroscopies, IINS gives access to all vibrational modes without any selection rules. Therefore, we have assigned this peak to the out-of-plane CH mode arising from mode 17a (Wilson notation). Indeed, this mode is almost never observed by Raman or IR spectoscopies, especially in the case of *para*-substituted aromatic compounds. In our study, the inactivity of this mode may be surprising if one takes into account the symmetry of the dendrimers, and their point group as either C_3 or D_3. Indeed, the nonexclusion of Raman and IR active modes due to the lack of inversion point, for instance, should lead to a larger number of bands in both spectra. However, it can be assumed that the local environment of the *para*-substituted benzene ring retains a pseudosymmetry D_{2h}. Thus, it can be postulated that, in the studied dendrimers, the E2u mode (17a) in the benzene ring becomes locally Au, again Raman and IR inactive. Another point, which merits attention, concerns the difference between the IINS data of **1** and **2**. Logically, these differences are due to the modes originating from the butyl substituent on the crown. Thus, the new intense bands which appear on IINS spectra of **2** at 1300 and 1444 cm^{-1} are assigned, respectively, to the overlapping of the CH_3 antisymmetric deformation (methyl out-of-plane HCH deformation) and the CH_2 scissors, and the in-plane methylene twisting-rocking mode.

All other assignments can be found in Table 1, with the associated number in Wilson notation.

Oxidized Dendrimers. The studied dendrimers are electron-rich molecules characterized by a high lying HOMO level (with respect to the vacuum level) and a low value of the ionization potential (IP). As a consequence, they are readily oxidized, forming stable radical cations and consecutively higher cationic states.[42,56−58] This is clearly manifested in their cyclic voltammograms.[42,56,58−60] Dendrons of the first generation with alkoxy substituents give rise to three reversible redox couples in the potential range from ca. −0.2 to +0.6 V vs Fc/Fc^+, associated with three consecutive one-electron oxidations from a neutral molecule to a three cation.[54,56] We observe qualitatively the same behavior for **2** in cyclic voltammetry and differential scanning voltammetry, however, with the potential of each redox couple systematically shifted to slightly higher values by 0.15−0.20 V. This difference between **2** and its methoxy-substituted analogue is obviously related to higher electron donating properties of the alkoxy substituents as compared to the alkyl ones.

As evidenced by cyclic voltammetry, neutral dendrons of the second generation can be oxidized to hexacations through three consecutive one-electron oxidations, followed by a three-electron oxidation. For the methoxy-substituted counterpart of **3**, these four oxidations occur in the potential range from ca. −0.30 V to ca. +0.20 V vs Fc/Fc^+.[54,56] The voltammetric behavior of **3** is qualitatively very similar; again, the corresponding peaks are shifted to higher potentials by 0.15−0.20 V, as expected.

UV−vis spectra of neutral dendrimers are characterized by two strongly overlapping peaks in the vicinity of 310 and 340 nm. In Figure 5, the spectrum of **2** is shown as a representative example.

It has been previously demonstrated by the correlation of cyclic voltammetry, UV−vis/NIR spectroelectrochemistry, and EPR data that the oxidation of a given dendrimer to a radical cation results in a sharp decrease of the band at ca. 350 nm and a smaller decrease of the 310 nm band; however, this band overlaps with that originating from the reduced form of the oxidant. Concomitantly, two new bands appear: a narrow one at ca. 440 nm in the case of **2** and a broad one with a clear maximum in the near-infrared part of the spectrum (at 1158 nm for **2**). Oxidation to higher cationic states induces a hypsochromic shift of the lower energetic (infrared) peak to 1130 nm with a simultaneous decrease in the intensity of the higher energetic band (440 nm in the case of **2**).[42] These changes are clearly reproduced in the spectra presented in Figure 5. For **2** oxidized with 1 equiv of the oxidant, the spectrum is characteristic of the radical cation state, and for the dendrimer oxidized with 3 equiv of the oxidant, it corresponds to the tricationic state. Note also that there is very little difference between the spectra of the dendrimer oxidized with 3 and 4 equiv of the oxidant, indicating the stability of the tricationic state.

dx.doi.org/10.1021/jp502735s | J. Phys. Chem. B XXXX, XXX, XXX−XXX

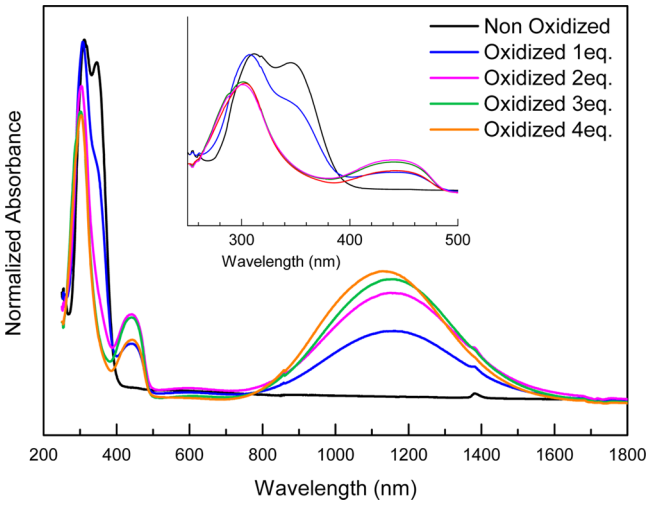

Figure 5. UV−vis spectra of thin films of **2** in its neutral state and oxidized with 1, 2, 3, and 4 equiv of tris(4-bromophenyl)ammonium hexachloroantimonate $[(BrC_6H_4)_3NSbCl_6]$.

These profound changes in the UV−vis/NIR spectra of the studied dendrimers have an important impact on the registered Raman spectra, since the resonance conditions are completely different for neutral molecules and for the oxidized (cationic) ones. In order to verify this effect, we have registered Raman spectra of thin films of **1** and **2** oxidized with either 1 or 3 equiv of the oxidant, yielding the lowest and highest cationic states, respectively. For **3**, we used 1 and 6 equiv of the oxidant. In the subsequent text, the corresponding samples will be termed "partially" and "fully" oxidized.

The effect of the excitation line energy on the resulting Raman spectra is demonstrated in Figure 6, where the case of fully oxidized **2** is used as an instructive example. For partially oxidized **2** and partially and fully oxidized **1**, the observed changes are very similar and the corresponding spectra can be found in the Supporting Information (Figures S1−S4).

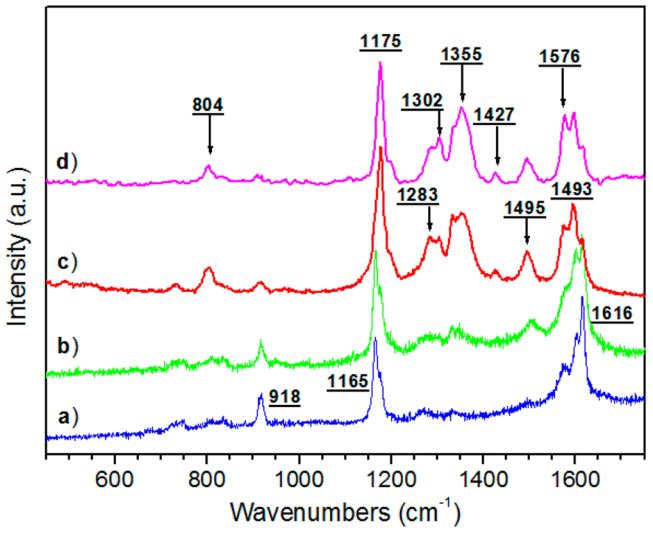

Figure 6. Raman spectra of **2** oxidized with 3 equiv of the oxidant ("fully oxidized") registered using different excitation lines: (a) blue line 458 nm; (b) green line 514 nm; (c) red line 647 nm; (d) Fourier transform Raman spectrum, infrared line 1064 nm.

In principle, one could expect a resonance enhancement of the spectral lines for λ_{exc} = 458 nm, since it matches in energy the oxidation-induced small absorption band at 440 nm. However, this absorption band does not yield any resonance, since using the blue excitation yields spectra of poor quality with two dominant lines characteristic of neutral amines (at 1611 and 1170 cm^{-1}). This means that vibrations from these parts of the dendrimer which do not bear positive charge are preferentially detected. Peaks originating from the charged (cationic) parts are present as broad, poorly resolved features in the spectral range between 1200 and 1600 cm^{-1}. Thus, the blue excitation line is of little use for investigating either neutral or oxidized (charged) forms of the discussed dendrimers.

With increasing wavelength of the excitation line from blue (λ_{exc} = 458 nm) to green (λ_{exc} = 514 nm) to red (λ_{exc} = 647 nm) to infrared (λ_{exc} = 1064 nm), the quality of the spectrum increases and the bands originating from the oxidized (charged) parts of **2** grow in intensity. For the infrared excitation line, they dominate the spectrum. This indicates that the lower energetic, oxidation-induced NIR band contributes to the resonance effect, since its maximum at 1110 nm closely matches the energy of the excitation line (1064 nm).

In Figure 7, Raman spectra of neutral, partially oxidized, and fully oxidized **2** are compared. The corresponding spectra of **1** can be found in the Supporting Information (Figures S2−S4).

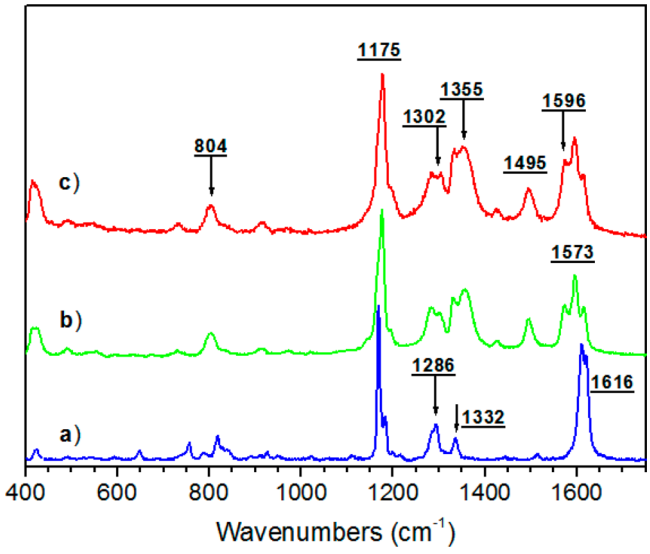

Figure 7. Raman spectra of (a) neutral **2** and **2** oxidized with (b) 1 and (c) 3 equiv of the oxidant ("partially oxidized" and "fully oxidized", respectively). λ_{exc} = 647 nm.

Before analyzing the spectra, it is instructive to discuss possible charge and spin configurations in the oxidized (charged) dendrimers. The use of 1 equiv of the oxidant imposes the presence of one radical cation per molecule of "partially" oxidized **2**, provided that the oxidation process occurs in a perfectly homogeneous way. Thus, semiquinone radical cation structure is expected in this case (Scheme 2). In "fully" oxidized **2**, three charges are introduced per molecule for a perfectly homogeneous oxidation. These three charges can be present as three radical cations of semiquinone structure or as one radical cation and one spinless dication, whose presence imposes the formation of a quinone-type ring (Scheme 2).

dx.doi.org/10.1021/jp502735s | J. Phys. Chem. B XXXX, XXX, XXX−XXX

Scheme 2. Chemical Structures of Triarylamine Dendrimer Oxidized to Radical Cation, Tri(radical cation), and Dication + Radical Cation

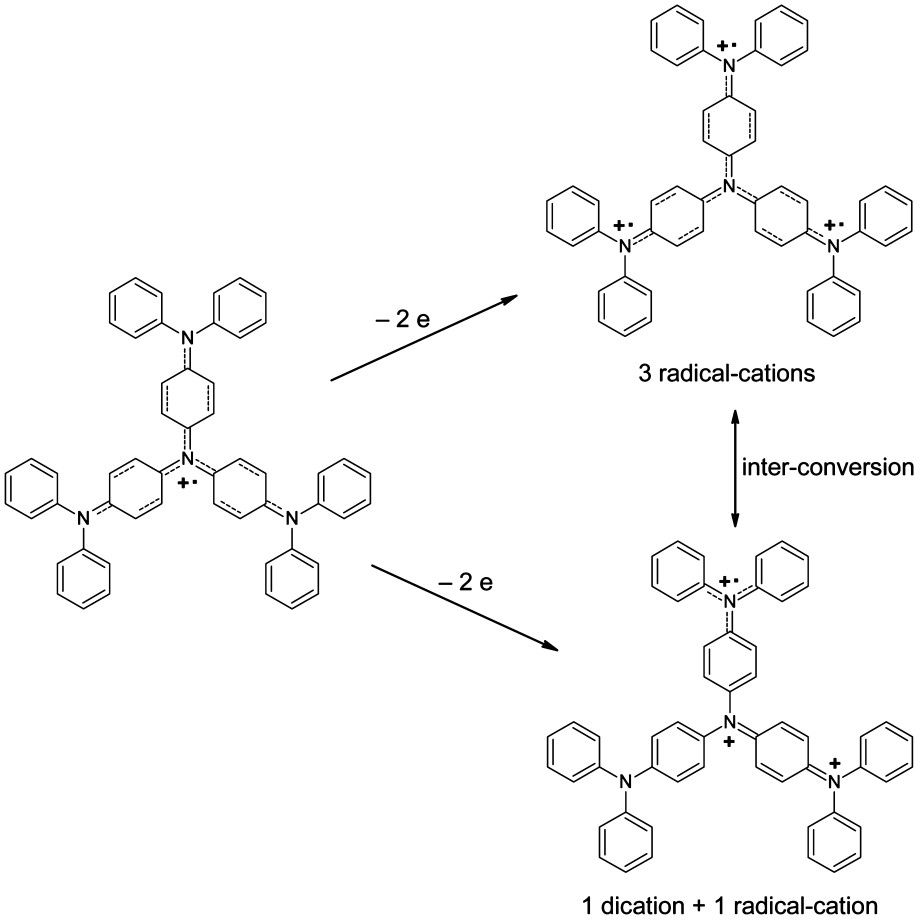

Table 2. Raman Frequencies (in cm^{-1}) of the Main Vibrational Modes of 1, 2, and 3 in Their Neutral and Highest Oxidation State

dendrimer 1		dendrimer 2		dendrimer 3		
exptl bands		exptl bands		exptl bands		
neutral	Ox	neutral	Ox	neutral	Ox	assignments
1610	1611	1616	1615	1616	1611	aromatic ring C—C stretch
	1584		1596		1582	semiquinonoid C═C stretch
	1569		1573			quinonoid ring, C═C stretch (dication)
	1487		1495	1499	1493	$C{=}N^{\circ+}$ stretch (spinless dication)
	1455		1427		1427	
	1357		1355		1348	$C{=}N^{\circ+}$ stretch (radical cation)
1333	1331	1333	1332	1344	1332	$C{=}N^{\circ+}$ stretch (radical cation)
1310	1299		1302		1303	C–N stretch (dication)
1287	1278	1286	1283	1280	1279	C–N stretch
	1173		1175		1176	C–H deformation (semiquinonoid ring)
1163	sh	1165	sh	1165	sh	C–H deformation (neutral and quinonoid ring)
	801		804		801	quinonoid ring deformation

Oxidation of **2** to the tricationic state involves profound spectral changes as revealed for the spectra obtained with either red or infrared excitation lines. First, the line at 1612 cm^{-1}, characteristic of the benzenoid ring in the neutral form of the molecule, diminishes in intensity on the expense of two lines at 1595 and 1571 cm^{-1}, which are usually attributed to C—C stretching in quinone or semiquinone rings. Concomitantly, the band originating from the C═N stretching at 1494 cm^{-1}, which is very weak in the spectrum of neutral **2** and indicates minute amounts of oxidation products, grows in intensity. Second, a new peak ascribed to the formation of radical cations in the oxidized form of the molecule appears at 1358 cm^{-1} and is accompanied by a second "radical cation" peak at 1333 cm^{-1}, already detected in the spectrum of the neutral form of **2**. Consistent with these changes, the band at 1289 cm^{-1}, attributed to the C—N stretching and clearly resolved in the spectrum of the neutral molecule, diminishes in intensity and in the case of the use of λ_{exc} = 1064 nm is present as a weak

dx.doi.org/10.1021/jp502735s | J. Phys. Chem. B XXXX, XXX, XXX–XXX

shoulder of the 1333 cm^{-1} band. Third, the peak attributed to the deformations of the amine group at 821 cm^{-1} in the spectrum of neutral **2** is shifted to 794 cm^{-1}, confirming the oxidation of the amine moiety. Finally, the band at 1171 cm^{-1} (C—H in-plane bending deformations in the aromatic ring) remains relatively unchanged with respect to the corresponding band in the spectrum of neutral **2**.

From this analysis, it appears clear that in the fully oxidized molecule both radical cations and quinone-type dications are present. This is perfectly consistent with the above outlined picture of the charge and spin storage configurations. However, the spectra of "partially" oxidized **2** also show the presence of a quinone-type dication, which should be absent if the oxidation was totally homogeneous. This finding may imply some nonhomogeneity in the oxidation process. However, the bands originating from quinone-type vibrations are strongly resonantly enhanced; therefore, the content of dications in the "partially" oxidized samples may be very low. Anyhow, resonant effects exclude in this case any quantitative estimation.

Our attempts to register Raman spectra of "fully" oxidized **3** were unsuccessful, independently of the excitation line used. The spectra of "partially" oxidized samples were very similar to those obtained for "partially" oxidized **1** and **2**. In Figure 8, its

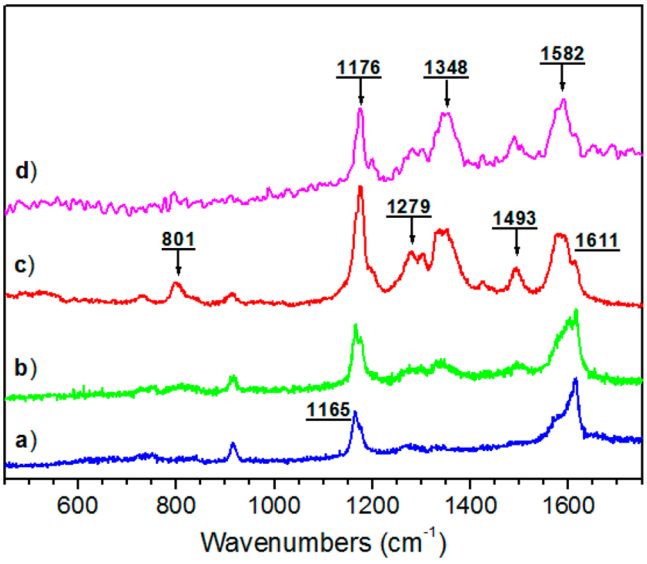

Figure 8. Raman spectra of **3** oxidized with 1 equiv of the oxidant ("partially oxidized"), registered using different excitation lines: (a) blue line 458 nm; (b) green line 514 nm; (c) red line 647 nm; (d) Fourier transform Raman spectrum, infrared line 1064 nm.

representative spectra, obtained for different λ_{exc} values, are presented. They can be interpreted in the same manner as the spectra of **2**. One should however note that the bands attributed to the presence of radical cations, in the spectral range 1330−1350 cm^{-1}, are relatively more intensive than in other cases. This may imply more homogeneous oxidation. However, the resonance effects exclude any quantitative approach.

CONCLUSIONS

To conclude, two families of dendrimers based on triphenylamine units were synthesized with two different crowns. On the basis of the geometries and the symmetry point groups of these compounds, obtained by applying semiempirical quantum chemistry methods, assignments of the main incoherent inelastic neutron scattering (IINS) bands in the 60−240 meV range were proposed in relation to the experimentally observed Raman and IR bands. To support these interpretations, numerical vibrational models of the studied compounds, based on the general valence force field method (GVFF), were established which additionally corroborated the proposed assignments. Moreover, the activity/inactivity of particular modes in different spectroscopies (IINS, Raman, IR) could be explained through symmetry considerations and taking into account the IINS cross section.

Raman spectroscopy was also applied to the investigations of the vibrational properties of cationic (oxidized) forms of these dendrimers. The obtained results allowed us to formulate the following conclusions. First, Raman spectra registered at different oxidation levels of the dendrimers strongly depended on the position of the excitation line with respect to their electronic spectrum. In particular: (1) the blue (458 nm) excitation line turned out to be insensitive toward the radical cationic and cationic forms of these compounds and revealed only the presence of unoxidized segments or unmodified aromatic rings from the crown. (2) The use of the red (647 nm) and infrared (1064 nm) excitation lines allowed for an unambiguous monitoring of the oxidation reaction, showing at the same time the formation of semiquinoid and quinoid segments in the cationic forms of the molecules. Finally, from these experimental observations, and based on the assignments of the Raman bands established for neutral molecules, it was possible to propose a mechanism of their oxidation to cationic forms, consistent with the experimental findings.

EXPERIMENTAL SECTION

Characterization Techniques. ^{1}H and ^{13}C NMR spectra were recorded on a Varian Mercury (400 and 100 MHz) spectrometer and referenced with respect to TMS and solvents. IR spectra were monitored on a Bio-RAD FTS-165 spectrometer using KBr pellets. UV−vis/NIR spectra were registered using a Cary 5000 (Varian) spectrometer. Mass spectra were measured by the EI method on an AMD 604 mass spectrometer. All synthesized compounds studied were subject to C, H, N, and Br elemental combustion analysis.

Reagents. Tris(4-bromophenyl)amine, 4-butylaniline, 4-butylbromobenzene, diphenylamine, palladium acetate, Pd-$(OAc)_2$, tris-*tert*-butylphosphine, *t*-Bu_3P, 2,2′-bis-(diphenylphosphino)-1,1′-binaphtyl, BINAP, sodium *tert*-butoxide, *t*-BuONa, di-*tert*-butyl dicarbonate, trifluoroacetic acid, tris(4-bromophenyl)amminium hexachloroantimonate, TBA·$SbCl_6$ anhydrous toluene, anhydrous dichloromethane, and anhydrous acetonitrile were purchased from Aldrich.

Di-(4-butylphenyl)amine was prepared according to ref 61.

All glassware was oven-dried, assembled hot, and cooled under a dry argon stream before use. All reactions were performed under dry argon.

The dendrimers were prepared according to the procedure described by Ito et al.[42] Below, we give the detailed description of the preparation of dendrimer **2** as an example.

Dendrimer ***1***. ^{1}H NMR (400 MHz, C_6D_6) δ, 7.12 (d, J = 8.4 Hz, 12H), 7.06−7.02 (m, 18H), 6.95 (d, J = 9.2 Hz, 6H), 6.82 (t, J = 7.4 Hz, 6H). ^{13}C NMR (100 MHz, C_6D_6) δ, 148.4, 143.5, 143.0, 129.5, 126.0, 125.1, 124.1, 122.7. IR (cm^{-1}): 3033, 2953, 2924, 2871, 1589, 1502, 1493, 1308, 1270, 1172, 1074, 820, 752, 695. Anal. Calcd for $C_{54}H_{42}N_4$: C, 86.86; H, 5.63; N, 7.51. Found: C, 86.54; H, 5.56; N, 7.27.

dx.doi.org/10.1021/jp502735s | J. Phys. Chem. B XXXX, XXX, XXX−XXX

Dendrimer 2. Di-(4-butylphenyl)amine, 0.927 g (3.3 mmol); tris(4-bromophenyl)amine, 0.482 g (1 mmol); sodium *tert*-butoxide, 0.346 g (3.6 mmol); palladium acetate, 20.2 mg (0.09 mmol); and *t*-Bu_3P, 54.6 mg (0.27 mmol) were dissolved in 15 mL of dry toluene under an argon atmosphere. The reaction mixture was stirred and heated at 110 °C for 12 h. The reaction mixture was then cooled to room temperature and washed with 30 mL of distilled water. The aqueous phase was extracted with three 5 mL portions of diethyl ether. The organic layers were combined and dried over $MgSO_4$. Removal of the solvents followed by chromatography on silica gel with hexanes/CH_2Cl_2 (2:1) resulted in a yellow solid. The resulting solid was recrystallized from THF/ethanol to give 0.95 g of **2** as a slightly yellow powder (yield 88%).

^{1}H NMR (400 MHz, C_6D_6) δ, 7.18 (d, J = 8.4 Hz, 12H), 7.06 (d, J = 2.8 Hz, 12H), 6.95 (d, J = 8.4 Hz, 12H), 2.43 (t, J = 7.6 Hz, 12H), 1.52−1.44 (m, 12H), 1.29−1.20 (m, 12H), 0.84 (t, J = 7.4 Hz, 18H). ^{13}C NMR (100 MHz, C_6D_6) δ, 146.5, 143.5, 143.1, 137.1, 129.6, 125.2, 125.1, 124.4, 35.1, 33.9, 22.4, 13.9. IR (cm^{-1}): 3027, 2956, 2927, 2871, 1505, 1466, 1306, 1267, 1114, 1016, 827. Anal. Calcd for $C_{78}H_{92}N_4$: C, 86.51; H, 8.32; N, 5.17. Found: C, 86.34; H, 8.19; N, 5.23. m/z = 1082.8.

Dendrimer 3. ^{1}H NMR (400 MHz, C_6D_6) δ, 7.18 (d, J = 8.4 Hz, 24H), 7.07 (s, 36H), 6.95 (d, J = 8.4 Hz, 24H), 2.42 (t, J = 7.6 Hz, 24H), 1.52−1.44 (m, 24H), 1.28−1.20 (m, 24H), 0.84 (t, J = 7.2 Hz, 36H). IR (cm^{-1}): 3027, 2956, 2927, 2871, 1505, 1466, 1306, 1267, 1114, 1016, 827. Anal. Calcd for $C_{174}H_{192}N_{10}$: C, 86.28; H, 7.93; N, 5.79. Found: C, 85.91; H, 8.06; N, 5.80.

Oxidation Procedure. The chemical oxidation of the dendrimers was carried out in an argon atmosphere. In a typical procedure, 6.5 × 10^{-5} mol of the dendrimer was dissolved in 2.2 mL of THF and then oxidized with the appropriate amount of tris(4-bromophenyl)amminium hexachloroantimonate, TBA·$SbCl_6$, in acetonitrile solution. The solution of the oxidized dendrimer was stirred under an argon atmosphere for 10 min. The solvents were evaporated in a vacuum, and the sample was dried in a vacuum to constant mass.

Inelastic Incoherent Neutron Scattering. Inelastic incoherent neutron scattering measurements in the 20−340 meV energy transfer range were carried out on a triple axis IN1 spectrometer at ILL (Grenoble). The spectrometer was used in the configuration involving a Cu_{220} crystal monochromator (λ = 1278 Å) equipped with a 60′ collimator. The analyzer was a BeF crystal. The samples were mounted in an aluminum foil flat container which was placed at 90° respectively to the incident beam. All spectra were recorded at 14 K. In such a configuration, the expected energy resolution was around 5.5 meV for small energy transfers in between 20 and 140 meV and then it linearly decreased to 7.5 meV for a 250 meV energy transfer.

A brief description of the neutron scattering theory can be found in the Supporting Information.

Raman Spectroscopy. Raman spectra of neutral and oxidized dendrimers were recorded on a Jobin-Yvon T64000 spectrometer (λ_{exc} = 457, 514, and 647 nm, laser power = 10 mW, 2 μm diameter spot, typical exposure times 60 s) or on a FT Raman Bruker RFS 100 spectrometer with the near-IR excitation line (1064 nm, laser power = 50 mW).

■ ASSOCIATED CONTENT

Ⓢ Supporting Information

A brief description of the neutron scattering theory; calculated bond lengths and angles, main force constants, and modeling Cartesian displacements (Chart S1a, b, and c); and Raman spectra of **2** (partially oxidized) and **1** (partially and fully oxidized). This material is available free of charge via the Internet at http://pubs.acs.org.

■ AUTHOR INFORMATION

Corresponding Authors

*E-mail: ikulsz@ch.pw.edu.pl.

*E-mail: Guy.Louarn@cnrs-imn.fr.

Present Address

⊥Institute of Computational Physics, Zurich University of Applied Sciences, Wildbachstrasse 21, CH-8401 Winterthur, Switzerland.

Notes

The authors declare no competing financial interest.

■ ACKNOWLEDGMENTS

I.K.-B., A.P., and L.S. wish to acknowledge financial support from National Centre of Science in Poland (NCN, Grant No. UMO-2011/01/B/ST5/03903). ILL is acknowledged for neutron beam time allocated for this work. Alexandre Ivanov is acknowledged for his assistance for measurements on IN1 at ILL. M.S. wishes to acknowledge CEA for a Ph.D. scholarship. L. Monestier and M. Bailo Diallo are thanked for their contributions during their Master trainings in CEA-Grenoble.

■ REFERENCES

(1) Lau, T.; Lorenz, E.; Koyuncu, M. Lifetime of Poly(triaryl amine) Based Organic Field Effect Transistors under Different Environmental Conditions. *Jpn. J. Appl. Phys.* **2013**, *52*, 041601−041605.

(2) Rybakiewicz, R.; Zapala, J.; Djurado, D.; Nowakowski, R.; Toman, P.; Pfleger, J.; Verilhac, J. M.; Zagorska, M.; Pron, A. Naphthalene Bisimides Asymmetrically and Symmetrically N-substituted with Triarylamine−Comparison of Spectroscopic, Electrochemical, Electronic and Self-Assembly Properties. *Phys. Chem. Chem. Phys.* **2013**, *15*, 1578−1587.

(3) Diallo, A. K.; Metri, N.; Brunel, F.; Sallenave, X.; Goubard, F.; Margeat, O.; Ackermann, J.; Videlot-Ackermann, C. A Star-Shaped Molecule as Hole Transporting Material in Solution-Processed Thin-Film Transistors. *Synth. Met.* **2013**, *184*, 35−40.

(4) Song, Y. B.; Di, C. A.; Yang, X. D.; Li, S. P.; Xu, W.; Liu, Y. Q.; Yang, L. M.; Shuai, Z. G.; Zhang, D. Q.; Zhu, D. B. A Cyclic Triphenylamine Dimer for Organic Field-Effect Transistors with High Performance. *J. Am. Chem. Soc.* **2006**, *128*, 15940−15941.

(5) Lee, J.; Cho, S.; Yang, C. Highly Reproducible Organic Field-Effect Transistor from Pseudo 3-Dimensional Triphenylamine-Based Amorphous Conjugated Copolymer. *J. Mater. Chem.* **2011**, *21*, 8528−8531.

(6) Zhao, Z. J.; Li, Z. F.; Lam, J. W. Y.; Maldonato, J. L.; Ramos-Ortiz, G.; Liu, Y.; Yuan, W. Z.; Xu, J. B.; Miao, Q.; Tang, B. Z. High Hole Mobility of 1,2-bis[4-(Diphenylamino)Biphenyl-4-yl]-1,2-Diphenylethene in Field Effect Transistor. *Chem. Commun.* **2011**, *47*, 6924−6926.

(7) Cravino, A.; Roquet, S.; Aleveque, O.; Leriche, P.; Frere, P.; Roncali, J. Triphenylamine-Oligothiophene Conjugated Systems as Organic Semiconductors for Opto-Electronics. *Chem. Mater.* **2006**, *18*, 2584−2590.

(8) Yasuda, T.; Shinohara, Y.; Ishi-i, T.; Han, L. Y. Use of Benzothiadiazole−Triphenylamine Amorphous Polymer for Reproducible Performance of Polymer−Fullerene Bulk-Heterojunction Solar Cells. *Org. Electron.* **2012**, *13*, 1802−1808.

(9) Bian, L. Y.; Yang, D.; Yin, L. M.; Zhang, J.; Tang, W. H. Carbazole Substituted Triphenylamine and Diketopyrrolopyrrole Alternating Copolymer for Photovoltaic Cells. *Macromol. Chem. Phys.* **2013**, *214*, 2136−2143.
(10) Roquet, S.; Cravino, A.; Leriche, P.; Aleveque, O.; Frere, P.; Roncali, J. Triphenylamine-Thienylenevinylene Hybrid Systems with Internal Charge Transfer as Donor Materials for Heterojunction Solar Cells. *J. Am. Chem. Soc.* **2006**, *128*, 3459−3466.
(11) Zhang, Z. G.; Liu, Y. L.; Yang, Y.; Hou, K. Y.; Peng, B.; Zhao, G. J.; Zhang, M. J.; Guo, X.; Kang, E. T.; Li, Y. F. Alternating Copolymers of Carbazole and Triphenylamine with Conjugated Side Chain Attaching Acceptor Groups: Synthesis and Photovoltaic Application. *Macromolecules* **2010**, *43*, 9376−9383.
(12) Deng, D.; Shen, S. L.; Zhang, J.; He, C.; Zhang, Z. J.; Li, Y. F. Solution-Processable Star-Shaped Photovoltaic Organic Molecule with Triphenylamine Core and Thieno [3, 2-b] Thiophene−Dicyanovinyl Arms. *Org. Electron.* **2012**, *13*, 2546−2552.
(13) Deng, D.; Yang, Y.; Zhang, J.; He, C.; Zhang, M. J.; Zhang, Z. G.; Zhang, Z. J.; Li, Y. F. Triphenylamine-Containing Linear DAD Molecules with Benzothiadiazole as Acceptor Unit for Bulk-Heterojunction Organic Solar Cells. *Org. Electron.* **2011**, *12*, 614−622.
(14) Hu, B. B.; Chen, X. P.; Wang, Y. F.; Lu, P.; Wang, Y. G. Structure-Property Investigations of Substituted Triarylamines and their Applications as Fluorescent pH Sensors. *Chem.—Asian J.* **2013**, *8*, 1144−1151.
(15) Shang, H. X.; Fan, H. J.; Liu, Y.; Hu, W. P.; Li, Y. F.; Zhan, X. W. A Solution Processable Star Shaped Molecule for High Performance Organic Solar Cells. *Adv. Mater.* **2011**, *23*, 1554−1557.
(16) Kwon, J.; Kim, M. K.; Hong, J. P.; Lee, W.; Lee, S.; Hong, J. I. A Multifunctional Material Based on Triphenylamine and a Naphthyl Unit for Organic Light-Emitting Diodes, Organic Solar Cells, and Organic Thin-Film Transistors. *Bull. Korean Chem. Soc.* **2013**, *34*, 1355−1360.
(17) Zhan, Y.; Peng, J.; Ye, K. Q.; Xue, P. C.; Lu, R. Pyrene Functionalized Triphenylamine-Based Dyes: Synthesis, Photophysical Properties and Applications in OLEDs. *Org. Biomol. Chem.* **2013**, *11*, 6814−6823.
(18) Huang, J. H.; Su, J. H.; Li, X.; Lam, M. K.; Fung, K. M.; Fan, H. H.; Cheah, K. W.; Chen, C. H.; Tian, H. Bipolar Anthracene Derivatives Containing Hole- and Electron-Transporting Moieties for Highly Efficient Blue Electroluminescence Devices. *J. Mater. Chem.* **2011**, *21*, 2957−2964.
(19) Jiang, Z. Q.; Ye, T. L.; Yang, C. L.; Yang, D. Z.; Zhu, M. R.; Zhong, C.; Qin, J. G.; Ma, D. G. Star-Shaped Oligotriarylamines with Planarized Triphenylamine Core: Solution-Processable, High-Tg Hole-Injecting and Hole-Transporting Materials for Organic Light-Emitting Devices. *Chem. Mater.* **2011**, *23*, 771−777.
(20) Jiang, W.; Yang, W.; Ban, X. X.; Huang, B.; Dai, Y. Q.; Sun, Y. M.; Duan, L.; Qiu, Y. Synthesis of New Bipolar Materials Based on Diphenylphosphine Oxide and Triphenylamine Units: Efficient Host for Deep-Blue Phosphorescent Organic Light-Emitting Diodes. *Tetrahedron* **2012**, *68*, 9672−9678.
(21) Iwan, A.; Sek, D. Polymers with Triphenylamine Units: Photonic and Electroactive Materials. *Prog. Polym. Sci.* **2011**, *36*, 1277−1325.
(22) Tao, Y. T.; Yang, C. L.; Qin, J. G. Organic Host Materials for Phosphorescent Organic Light-Emitting Diodes. *Chem. Soc. Rev.* **2011**, *40*, 2943−2970.
(23) Anderson, J. D.; McDonald, E. M.; Lee, P. A.; Anderson, M. L.; Ritchie, E. L.; Hall, H. K.; Hopkins, T.; Mash, E. A.; Wang, J.; Padias, A.; et al. Electrochemistry and Electrogenerated Chemiluminescence Processes of the Components of Aluminum Quinolate/Triarylamine, and Related Organic Light-Emitting Diodes. *J. Am. Chem. Soc.* **1998**, *120*, 9646−9655.
(24) Bender, T. P.; Graham, J. F.; Duff, J. M. Effect of Substitution on the Electrochemical and Xerographic Properties of Triarylamines: Correlation to the Hammett Parameter of the Substituent and Calculated HOMO Energy Level. *Chem. Mater.* **2001**, *13*, 4105−4111.
(25) Xiao, H.; Leng, B.; Tian, H. Hole Transport Triphenylamine−Spirosilabifluorene Alternating Copolymer: Synthesis and Optical, Electrochemical and Electroluminescent Properties. *Polymer* **2005**, *46*, 5707−5713.
(26) Cheng, H. C.; Chiu, K. Y.; Tu, Y. J.; Yang, T. F.; Su, Y. O. Electrochemically Controlled Multiple Hydrogen Bonding between Triarylamines and Imidazoles. *Org. Lett.* **2013**, *15*, 3868−3871.
(27) Casalbore-Miceli, G.; Esposti, A. D.; Fattori, U.; Marconi, G.; Sabatini, C. A Correlation between Electrochemical Properties and Geometrical Structure of some Triarylamines Used as Hole Transporting Materials in Organic Electroluminescent Devices. *Phys. Chem. Chem. Phys.* **2004**, *6*, 3092−3096.
(28) Song, Y.; Di, C.; Xu, W.; Liu, Y.; Zhang, D.; Zhu, D. New Semiconductors Based on Triphenylamine with Macrocyclic Architecture: Synthesis, Properties and Applications in OFETs. *J. Mater. Chem.* **2007**, *17*, 4483−4491.
(29) Tang, C. W.; Van Slyke, S. A. Organic Electroluminescent Diodes. *Appl. Phys. Lett.* **1987**, *51*, 913−915.
(30) Seo, E. T.; Nelson, R. F.; Fritsch, J. M.; Marcoux, I. S.; Leedy, D. W.; Adams, R. N. Anodic Oxidation Pathways of Aromatic Amines. Electrochemical and Electron Paramagnetic Resonance Studies. *J. Am. Chem. Soc.* **1966**, *88*, 3498−3503.
(31) Connelly, N. G.; Geiger, W. E. Chemical Redox Agents for Organometallic Chemistry. *Chem. Rev.* **1996**, *96*, 877−910.
(32) Shirota, Y. Organic Materials for Electronic and Optoelectronic Devices. *J. Mater. Chem.* **2000**, *10*, 1−25.
(33) Louie, J.; Hartwig, J. F.; Fry, A. J. Discrete High Molecular Weight Triarylamine Dendrimers Prepared by Palladium-Catalyzed Amination. *J. Am. Chem. Soc.* **1997**, *119*, 11695−11696.
(34) Lambert, C.; Amthor, S.; Schelter, J. From Valence Trapped to Valence Delocalized by Bridge State Modification in bis(Triarylamine) Radical Cations: Evaluation of Coupling Matrix Elements in a Three-Level System. *J. Phys. Chem. A* **2004**, *108*, 6474−6486.
(35) Lambert, C.; Nöll, G. The Class II/III Transition in Triarylamine Redox Systems. *J. Am. Chem. Soc.* **1999**, *121*, 8434−8442.
(36) Lancarter, K.; Odom, S. A.; Thayumanavan, S.; Marder, S. R.; Bredas, J. L.; Coropceanu, V.; Barlow, S. Intramolecular Electron-Transfer Rates in Mixed-Valence Triarylamines: Measurement by Variable-Temperature ESR Spectroscopy and Comparison with Optical Data. *J. Am. Chem. Soc.* **2009**, *131*, 1717−1723.
(37) Amthor, S.; Noller, B.; Lambert, C. UV/Vis/NIR Spectral Properties of Triarylamines and Their Corresponding Radical Cations. *Chem. Phys.* **2005**, *316*, 141−152.
(38) Lovesey, S. W. *Theory of Neutron Scattering from Condensed Matter*; Oxford University Press: Oxford, U.K., 1984.
(39) Kim, J-.S.; Ho, P. K. H.; Murphy, C. E.; Seeley, A. J. A. B.; Grizzi, I.; Burroughes, J. H.; Friend, R. H. Electrical Degradation of Triarylamine-Based Light-Emitting Polymer Diodes Monitored by Micro-Raman Spectroscopy. *Chem. Phys. Lett.* **2004**, *386*, 2−7.
(40) Zhang, K.; Wang, L.; Liang, Y.; Yang, S.; Liang, J.; Cheng, F.; Chen, J. A Thermally and Electrochemically Stable Organic Hole-Transporting Material with an Adamantane Central Core and Triarylamine Moieties. *Synth. Met.* **2012**, *162*, 490−496.
(41) Zhang, Y.; Sun, J.; Zhuang, G.; Ouyang, M.; Yu, Z.; Cao, F.; Pan, G.; Tang, P.; Zhang, C.; Ma, Y. Heating and Mechanical Force-Induced Luminescence on−off Switching of Arylamine Derivatives with Highly Distorted Structures. *J. Mater. Chem. C* **2014**, *2*, 195−200.
(42) Ito, A.; Sakamaki, D.; Ichikawa, Y.; Tanaka, K. Spin-Delocalization in Charged States of para-Phenylene-Linked Dendridic Oligoarylamines. *Chem. Mater.* **2011**, *23*, 841−850.
(43) Zhang, S. L. *Raman Spectroscopy and its Application in Nanostructures*; John Wiley & Sons: Chichester, U.K., 2012.
(44) Boyer, M. I.; Quillard, S.; Cochet, M.; Louarn, G.; Lefrant, S. RRS Characterization of Selected Oligomers of Polyaniline in situ Spectroelectrochemical Study. *Electrochim. Acta* **1999**, *44*, 1981−1987.
(45) Rai, G.; Kumar, A. K.; Rai, S. Infrared, Raman Spectra and DFT Calculations of Chlorine Substituted Anilines. *Vib. Spectrosc.* **2006**, *42*, 397−402.

(46) Quillard, S.; Louarn, G.; Lefrant, S.; MacDiarmid, A. G. Vibrational Analysis of Polyaniline: a Comparative Study of Leucoemeraldine, Emeraldine, and Pernigraniline Bases. *Phys. Rev. B* **1994**, *50*, 12496−12508.
(47) Dollish, F. R.; Fateley, W. G.; Bentley, F. F. *Characteristic Raman Frequencies of Organic Compounds*; John Wiley & Sons: New York, 1969.
(48) Cochet, M.; Louarn, G.; Quillard, S.; Buisson, J. P.; Lefrant, S. Theoretical and Experimental Vibrational Study of Emeraldine in Salt Form. Part II. *J. Raman Spectrosc.* **2000**, *31*, 1041−1049.
(49) Louarn, G.; Buisson, J. P.; Lefrant, S.; Fichou, D. Vibrational Studies of a Series of alpha-Oligothiophenes as Model Systems of Polythiophene. *J. Phys. Chem.* **1995**, *99*, 11399−11404.
(50) Cochet, M.; Louarn, G.; Quillard, S.; Boyer, M. I.; Buisson, J. P.; Lefrant, S. Theoretical and Experimental Vibrational Study of Polyaniline in Base Forms: Non Planar Analysis. Part I. *J. Raman Spectrosc.* **2000**, *31*, 1029−1039.
(51) Louarn, G.; Lapkowski, M.; Quillard, S.; Pron, A.; Lefrant, S. Vibrational Properties of Polyaniline Isotope Effects. *J. Phys. Chem.* **1996**, *100*, 6998−7006.
(52) Meijer, G.; Berden, G.; Meerts, W. L.; Hunziker, H. E.; de Vries, M. S.; Wendt, H. R. Spectroscopy on Triphenylamine and its Van Der Waals Complexes. *Chem. Phys.* **1992**, *163*, 209−222.
(53) Sobolev, A. N.; Belsky, V. K.; Romm, I. P.; Chernikova, N. Y.; Guryanova, E. N. Structural Investigation of the Triaryl Derivatives of the Group V Elements. IX. Structure of Triphenylamine, $C_{18}H_{15}N$. *Acta Crystallogr., Sect. C* **1985**, *41*, 967−971.
(54) Wilson, E. B., Jr. The Normal Modes and Frequencies of Vibration of the Regular Plane Hexagon Model of the Benzene Molecule. *Phys. Rev.* **1934**, *45*, 706−714.
(55) Varsányi, G. *Vibrational spectra of benzene derivatives*; Academic Press: New York, 1969; pp 17−84.
(56) Selby, T. D.; Kim, K. Y.; Blackstock, S. C. Patterned Redox Arrays of Polyarylamines I. Synthesis and Electrochemistry of a p-Phenylenediamine and Arylamino-Appended p-Phenylenediamine Arrays. *Chem. Mater.* **2002**, *14*, 1685−1690.
(57) Hirao, Y.; Ito, A.; Tanaka, K. Intramolecular Charge Transfer in a Star-Shaped Oligoarylamine. *J. Phys. Chem. A* **2007**, *111*, 2951−2956.
(58) Hirao, Y.; Ino, H.; Ito, A.; Tanaka, K.; Kato, T. High-Spin Radical Cations of a Dendridic Oligoarylamine. *J. Phys. Chem. A* **2006**, *110*, 4866−4872.
(59) Kim, K. V.; Hassenzahl, J. D.; Selby, T. D.; Szulczewski, G. J.; Blackstock, S. C. Patterned Redox Arrays of Polyarylamines II. Growth of Thin Films and Their Electrochemical Behavior. *Chem. Mater.* **2002**, *14*, 1691−1694.
(60) Li, J. C.; Kim, K. Y.; Blackstock, S. C.; Szulczewski, G. J. Patterned Redox Arrays of Polyarylamines III. Effect of Molecular Structure and Oxidation Potential on Film Morphology and Hole-Injection in Single-Layer Organic Diodes. *Chem. Mater.* **2004**, *16*, 4711−4714.
(61) Maurel, V.; Jouni, M.; Baran, P.; Onofrio, N.; Gambarelli, S.; Mouesca, J. M.; Djurado, D.; Dubois, L.; Jacquot, J. F.; Desfonds, G.; et al. Magnetic Properties of a Doped Linear Polyarylamine Bearing a High Concentration of Coupled Spins (S = 1). *Phys. Chem. Chem. Phys.* **2012**, *14*, 1399−1407.